International Journal of Modern Manufacturing Technologies
ISSN 2067–3604, Vol. XV, No. 3 / 2023
https://doi.org/ 10.54684/ijmmt.2023.15.3.155

ASSESSMENT OF PROPERTIES AND CORROSION RESISTENCE OF GALVANIZED STEEL WELDED WITH LASER BEAM

Agnieszka Rzeźnikiewicz[1], Jacek Górka[1] , Mateusz Przybyła[1], Monika Kciuk[2]

[1]Silesian University of Technology, Mechanical Engineering Faculty, Department of Welding Engineering, Konarskiego 18a, 44-100 Gliwice, Poland
[2]Silesian University of Technology, Mechanical Engineering Faculty, Department of Engineering Materials and Biomaterials, Konarskiego 18a, 44-100 Gliwice, Poland

Corresponding author: Agnieszka Rzeźnikiewicz, agnieszka.rzeznikiewicz@polsl.pl

Abstract: The paper describes the influence of laser welding parameters on the structure, mechanical properties and corrosion resistance of 1.2 mm thick galvanized sheets made of DC04 low-carbon steel. The tested test joints were made with a disc laser on a robotic laser welding station (TruLaser Robot 5120) with a TruDisk 12002 laser. In the laser welding process, butt welded joints were made without additional material with variable welding speed (linear welding energy from 30 to 45 J/mm). Welded joints were subjected to non-destructive tests (visual, magnetic-particle and radiographic tests), destructive tests (tensile strength, bend test, hardness test) and tests for corrosion resistance (corrosion potential test, using a three-electrode measuring system and a potentiostat - ATLAS 0531 EU galvanostat) by Atlas-Sollich and corrosion test in a salt chamber). The conducted tests have shown that it is possible to make connections that meet the criteria of ISO 15614-11. All made joints, regardless of the applied linear energy of welding, are characterized by high strength and plastic properties. It can be noticed that as the linear energy of welding increases, the weld seam and the heat-affected zone of the welded joints become wider. A joint made with higher linear energy has higher hardness and tensile strength than a joint made with lower linear energy. In the static tensile test, rupture occurred in the base material, regardless of the value of the linear energy of welding. In the bending test, regardless of the value of the linear energy of welding, the bending angle of 180 ° was achieved, without tears and scratches, the values of relative elongation ranged from 29% to 42%, which confirms the high plastic properties. A joint made with lower line energy has greater corrosion resistance than a joint made with higher line energy, but much lower than the native material. It can be assumed that during welding a part of the galvanic coating is removed or damaged.
Key words: body sheets, laser welding, linear welding energy, strength properties, corrosion resistance

1. INTRODUCTION

In the automotive industry, steel accounts for a significant proportion of a car's weight. Data from 2017 shows that steel and cast elements account for about 55%, the next group of materials is plastics, which account for about 11%, and aluminum alloys with a 9% share in the vehicle weight [1-7]. The development of the automotive industry is associated with an increased demand for new construction materials. Car manufacturers compete with each other and want to reach a growing group of recipients, so they try to meet the expectations of consumers regarding the increasingly better quality of products. Good quality has a positive effect on the safety of the vehicle, and also increases its level of reliability [8,9]. During manufacturing high-quality components, special attention should be paid to the quality of the welding joints. Spot welding technologies have been most often used to connect the car body, but laser welding technology is also increasingly chosen because of its advantages [10-13]. The car body constructor has only three parameters to combine in order to achieve an optimal solution - geometric shape, material and joining method - choosing the right joining technique is essential. This explains why new assembly technologies have recently gained a lot of interest and are becoming more and more popular replacing traditional welding methods [13-15].
The increasing requirements for service life and corrosion resistance have resulted in the use of zinc-coated steel body sheets in today's automotive industry. They are characterized by very high mechanical properties, and most importantly - thanks to the zinc coating of these sheets - high resistance to corrosion. Unfortunately, the process of joining these sheets is a significant technological problem. The evaporation temperature of zinc is 907°C, which causes porosity of the welds and loss of corrosion resistance in the joint area. Mechanically removing zinc before welding and reapplying where evaporation has occurred is a very costly process. In addition, in the process of zinc evaporation, there is a very large emission of zinc vapor, which has a bad effect on human health. The stability

of the optimal process parameters and the quality of the preparation of the joined edges are particularly important factors in laser welding. An increase in the welding speed causes narrowing of the width of the weld face, heat affected zone and root, while exceeding a certain value of the welding speed may cause weld non conformities in the performed joint, such as excessive root reinforcement, incompletely filled groove [13-17].

2. EXPERIMENTS

2.1. Materials

The aim of the work was to determine the effect of laser welding parameters on the structure, mechanical properties and corrosion resistance of galvanized sheets made of low-carbon steel DC04 with a thickness of 1.0 mm. DC04 steel is a low-carbon steel intended for cold forming, suitable for deep drawing. The applied zinc coatings protect the surface of the sheet against the corrosive effects of the external environment. This steel is used in the automotive industry to build car bodies. The chemical composition and properties of the tested material are presented in Tables 1 and 2, and the structure in Fig. 1.

Table 1. Chemical composition of DC04 steel

Chemical composition %			
C	P	S	Mn
≤0.08	0.03	0.03	0.40

Table 2. Selected properties of DC04 steel in tempered condition

Yield strength Re [MPa]	Tensile strength Rm [MPa]	Elongation A80 [%]	Hardness [HV]
Min 210	270 - 355	38	100 - 110

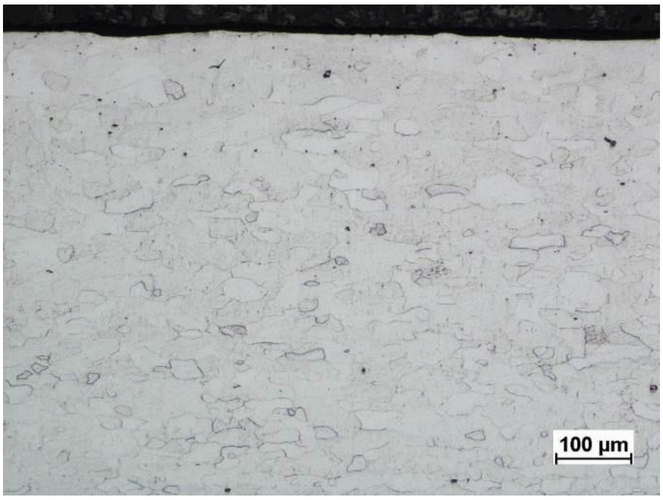

Fig. 1. Structure of the parent material

2.2. Welding process

Galvanized steel sheets were cut to size 300x150x1.0 mm. Then the samples were cleaned and degreased. The test joints were made with a disk laser on a robotic laser welding station (TruLaser Robot 5120) with a TruDisk 12002 laser. In the laser welding process, butt welds were made without additional material. The joints were made with a variable linear welding energy. The parameters of the welding process are presented in Table 3, a view of the weld face and root area in Fig. 2.

Table 3. Parameters of the welding process

Weld designation	Beam power [W]	Welding speed [m/min]	Welding linear energy [kJ/mm]
Joint 1	1500	3	0.3
Joint 2	1500	2	0.45

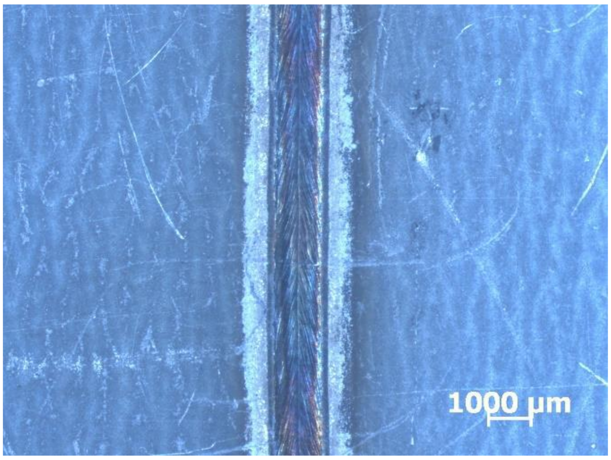

Joint 1 - the weld face

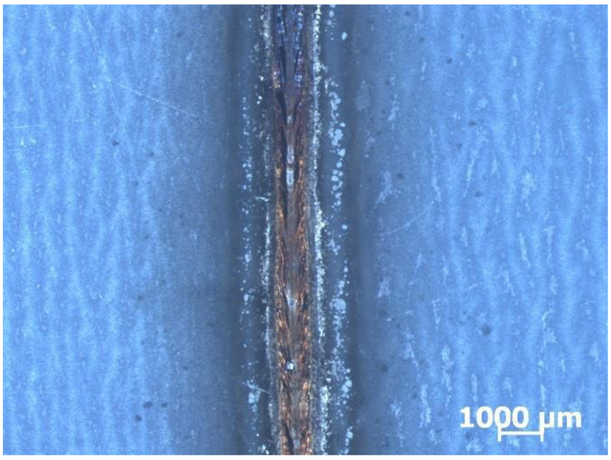

Joint 1 - the weld root

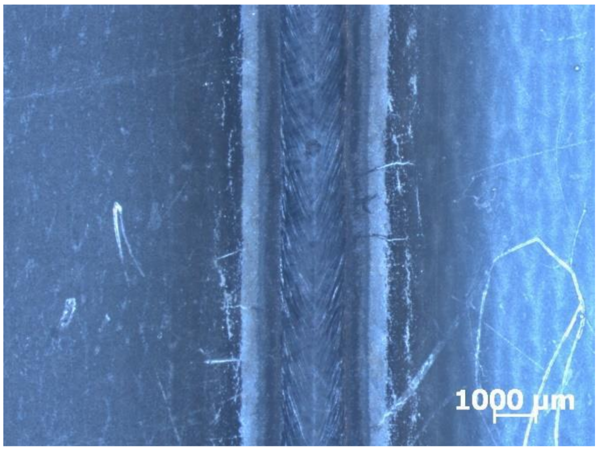

Joint 2 - the weld face

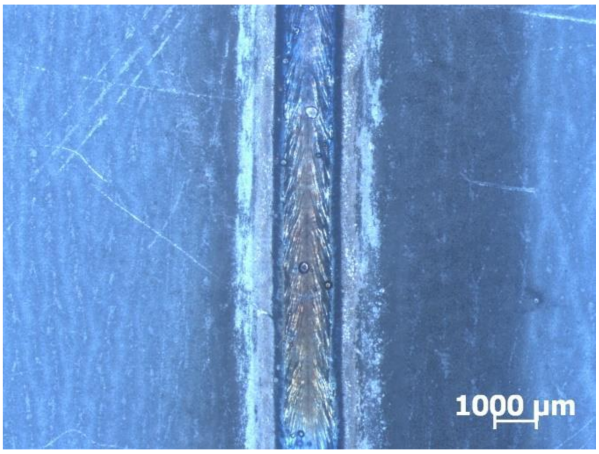

Joint 2 - the weld root

Fig 2. A view of the weld face and root area

2.3. Testing of welded joints

The obtained test joints were subjected to non-destructive tests:

- Visual tests according to EN ISO 17637:2017;
- Magnetic-particle tests according to EN ISO 3059:2013, EN ISO 9934-2:2015, EN ISO 9934-3:2015. MR 72 was used as a white contrasting base, the magnetic powder MR 76S was used to carry out the tests. The tests were carried out using a yoke electromagnet;
- X – ray examination according to EN ISO 17636:2013. An X-ray tube CERAM type 235 was used with a beam of X-rays with a diameter of d = 2 mm at a voltage U = 180 kV, current I = 3 mA, using reinforcing covers OW - 0.15 mm. The test results were recorded on AGFA type C5 photographic film, using the exposure time t = 2.3 min and the focal length f = 700 mm.

After non-destructive tests, the welded joint was subjected to destructive tests in the following scope:

- tensile strength tests according to EN ISO 6892-1:2020 on a ZWICK/ROELL Z 330RED testing machine on samples taken according to with PN-EN ISO 4136:2022;
- transverse bending test of the butt joint with stretching from the weld face side and bending test of the butt joint with stretching from the weld root side according to the PN-EN ISO 5173:2010 standard. Bending tests were carried out using a ZWICK/ROELL Z 330RED machine with an additional module for bending tests using a bending mandrel with a diameter of 10 mm;
- macroscopic metallographic examinations were performed on the Olympus SZX9 stereoscopic light microscope; test samples were etched in Adler;
- metallographic microscopic examinations were performed on a NIKON ECLIPSE MA100 light microscope; test samples were etched in nital;
- hardness measurement was carried out using Vickers 401MVD device by Wilson Wolpert, with a load of 200g;
- corrosive potential examination. As an electrolyte, a water solution of sodium chloride with a mass concentration of 3% was used, the reference electrode was saturated with AgCl electrode, while the anti -electrode was made of stainless steel;

• corrosion tests in the ASCOTT CC450IP salt chamber were carried out in accordance with PN-EN ISO 9227. The samples were placed in a salt chamber for 96h, where 5% of the fog of a salt water solution of sodium chloride was exposed, at 35 ° C and 100% humidity conditions;
• Fractographic tests after corrosive examinations, using the Zeiss Stereo Discovery V12 stereoscopic microscope at 100x enlargement.

3. RESULTS AND DISCUSSION

3.1. Non-destructive tests

Visual tests and magnetic-powder tests of the welded joints performed at the linear energy of 0.3 and 0.45 kJ/mm did not show any welding defects coming to the surface. All welded joints met the requirements of quality level B according to ISO 13919-1:2020. Also, macroscopic examinations did not show any welding non conformities in the area of the weld and HAZ (fig. 3).

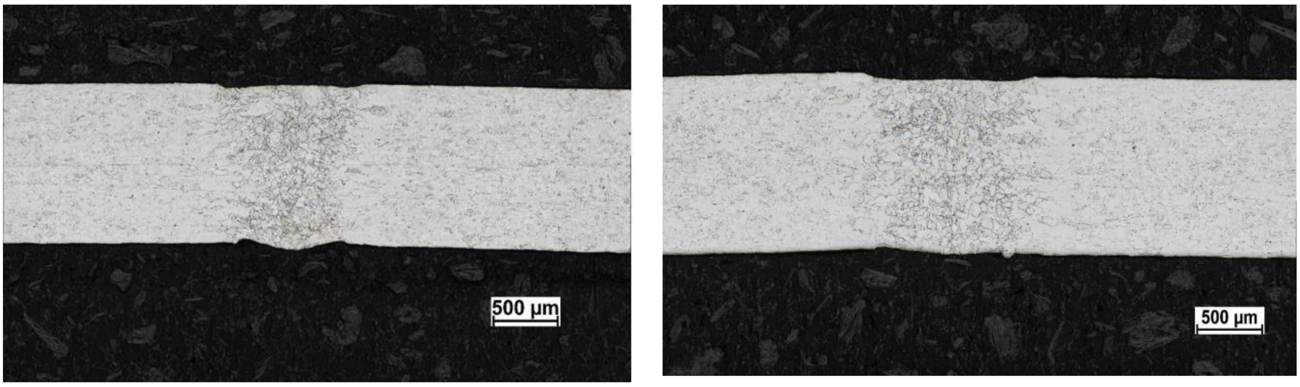

Joint 1 Joint 2

Fig. 3. Macrostructure of welded joints

3.2. Microscopic examination

Microscopic examinations in the weld area shows the influence of the welding linear energy on the structure and grain size in the weld area and HAZ. In the case of welds made with lower linear welding energy (0.3 kJ/mm), in addition to the ferritic-pearlitic structure, smaller grain can be observed. The proportion of ferrite in the weld increases with the increase of the welding linear energy. The area of the heat affected zone (HAZ) is characterized by grain size variability. In the HAZ area, the grain size increases with the increase in the welding linear energy, Fig. 4.

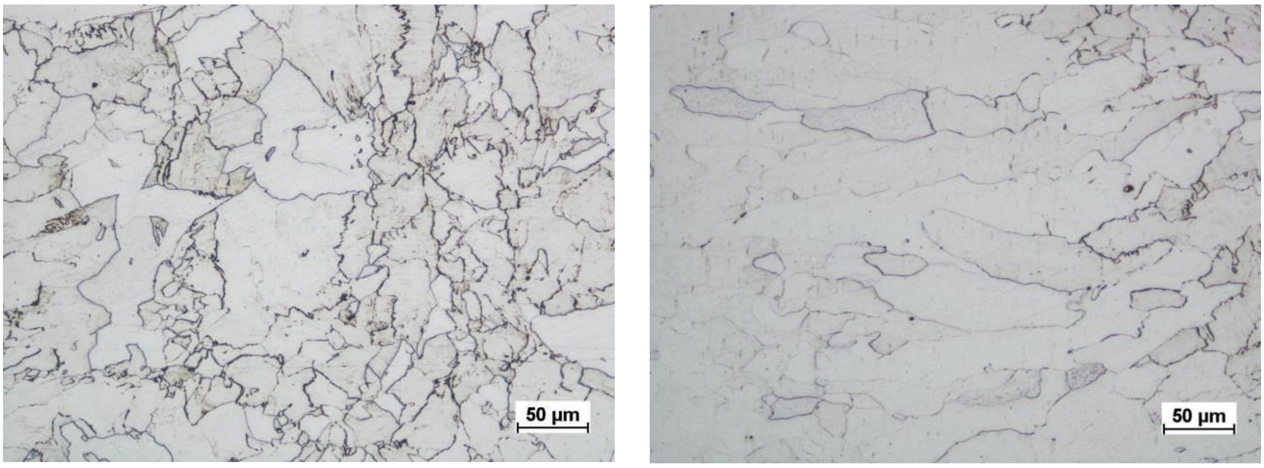

Weld (joint 1) HAZ (joint 1)

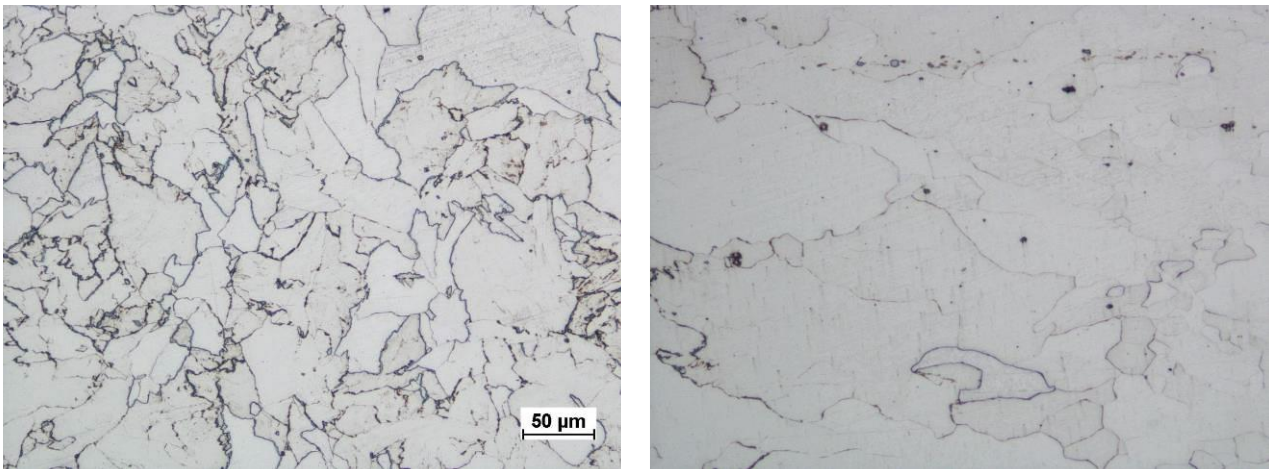

Weld (joint 2) HAZ (joint 2)

Fig. 4. Microstructure of welded joints made with variable linear welding energy

3.3. Hardness tests

The analysis of the results of hardness measurements confirmed the observations from metallographic microscopic examinations. The results of hardness measurements (Fig. 5) show the increase in hardness in the heat affected zone and in the weld in relation to the parent material, whose hardness was approx. 110 $HV_{0.2}$. The highest hardness value was obtained in the weld of joint 1 made with lower linear energy (0.3 kJ/mm), which is related to the smallest grain size. With the increase in the linear energy of welding, the value of the maximum hardness in the weld decreases to about 155 $HV_{0.2}$. In the area of HAZ, the obtained hardnesses are in the range of 125 to 145 $HV_{0.2}$ and decrease with the increase of the welding linear energy, which is related to the grain size, Fig. 5.

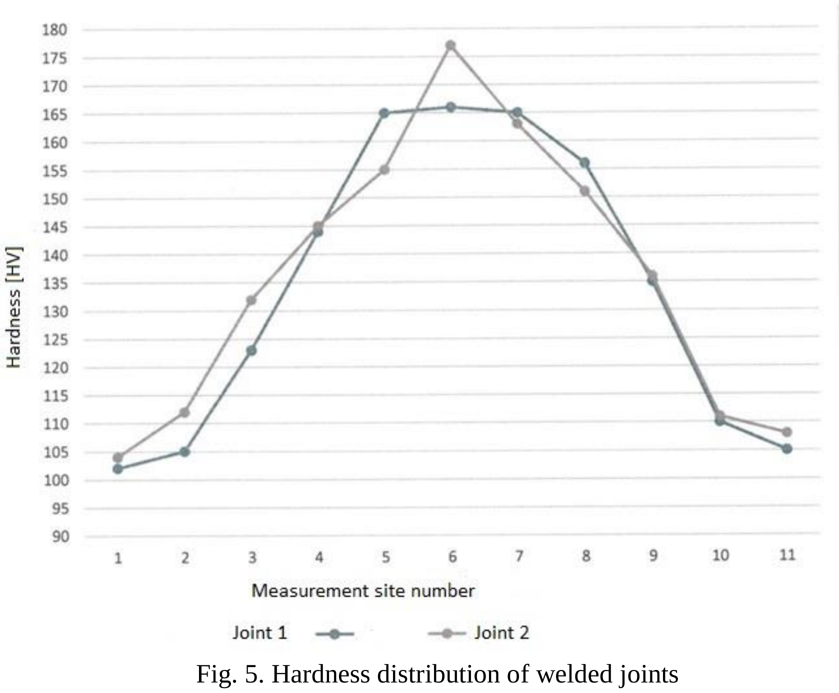

Fig. 5. Hardness distribution of welded joints

3.4. Static tensile tests

The conducted static tensile test showed that all joints are characterized by high tensile strength (at the level of 290 MPa), and the rupture occurred outside the area of the welded joint, Table 4, Fig. 6.

Table 4. The results of the static tensile strength

Weld designation	Tensile strength Rm, [MPa]	Elongation A_t, [%]	S_0 [mm^2]	Breaking point
Joint 1_1	289	40	10	BM*

Joint 1_2	290	42	10	BM
Joint 2_1	301	38	10	BM
Joint 2_2	298	38	10	BM

*BM – Base material

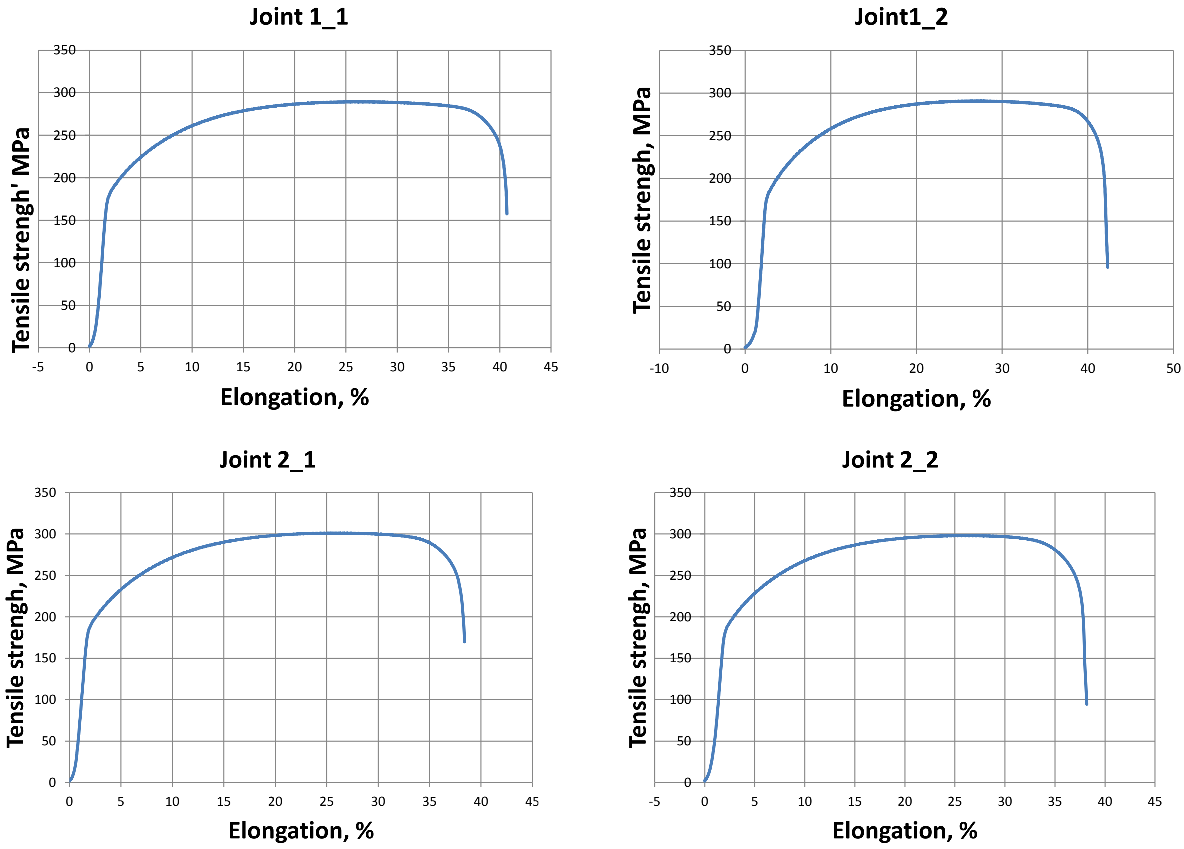

Fig. 6. Tensile strength diagram

3.5. Bending tests

The bending test made it possible to achieve a bending angle of 180°, both during bending from the face and root side of the joint, which proves the high plastic properties of the joint obtained, Fig. 7.

Face bend – joint 1 | Face bend – joint 2

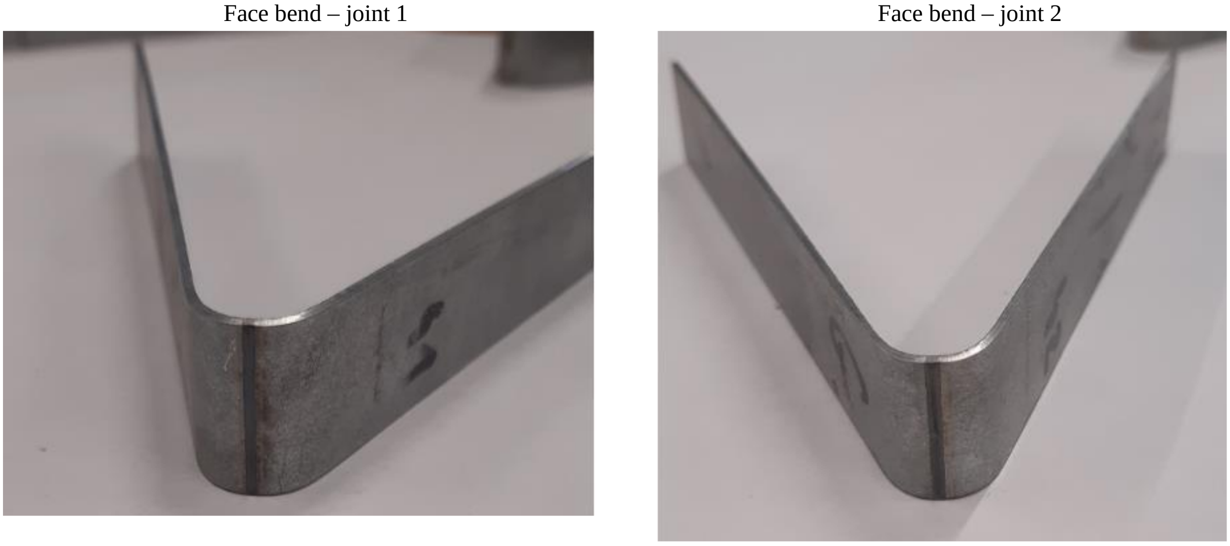

Root bend – joint 1 | Root bend – joint 2

Fig. 7. A view of the joints after bending test

3.6. Corrosion resistance tests

Electrochemical tests were used to assess the corrosion resistance of the tested material and the welded joint in the given corrosion conditions. Corrosion tests were carried out in a 3.5% NaCl environment simulating a seawater environment. The recording of the polarization curves started after the corrosion potential was determined after about one hour. The corrosion potential $Ekor$ of the parent material ranged from - 1.15V to - 0.951V. The value of polarization resistance during subsequent measurements was 3.1 kΩ, 4.08 kΩ and 2.2 kΩ, Fig. 8. The difference in resistance between the measurements may result from scratches, zinc coating losses.

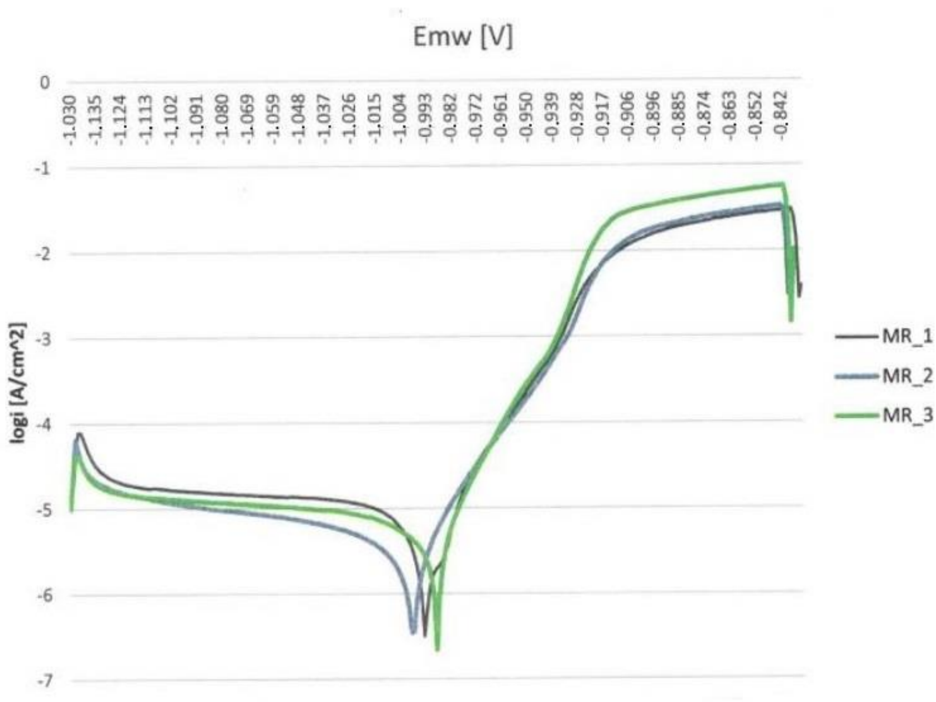

Fig. 8. Summary of the results of the potentiodynamic study of the parent material: MR_1 the first measurement, MR_2 the second measurement, MR_3 the third measurement of the parent material

The corrosion potential $Ekor$ of the joint welded with linear energy 0.3 kJ/mm ranged from - 0.99V to - 0.975V. The value of the polarization resistance was 2.43 kΩ for the first measurement and 1.04 kΩ for the second, Fig 9. The difference in the value of the polarization resistance may result from the fact that during the welding part of the galvanic coating was damaged or removed.

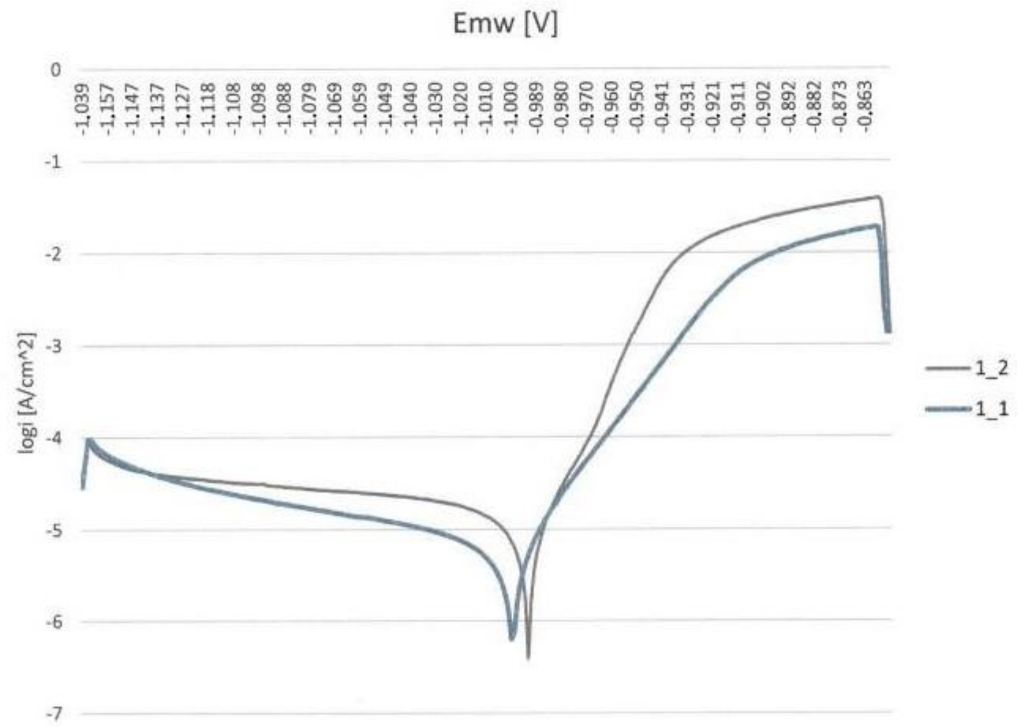

Fig. 9. Summary of the results of the potentiodynamic study of joint 1: 1_1 the first measurement, 1_2 the second measurement

In the case of a joint welded with a linear energy of 0.45 kJ/mm, the corrosion potential $Ekor$ ranged from - 1.0V to - 0.95V. The polarization resistance value was 483 Ω for the first measurement, 970 Ω for the second measurement and 1.7 kΩ for the third measurement, Fig. 10. The difference in resistance for this joint varies significantly because part of the galvanic coating was removed during the welding process. As in the case of joint 1, it can be seen that after reaching the critical value of the potential, passivation began.

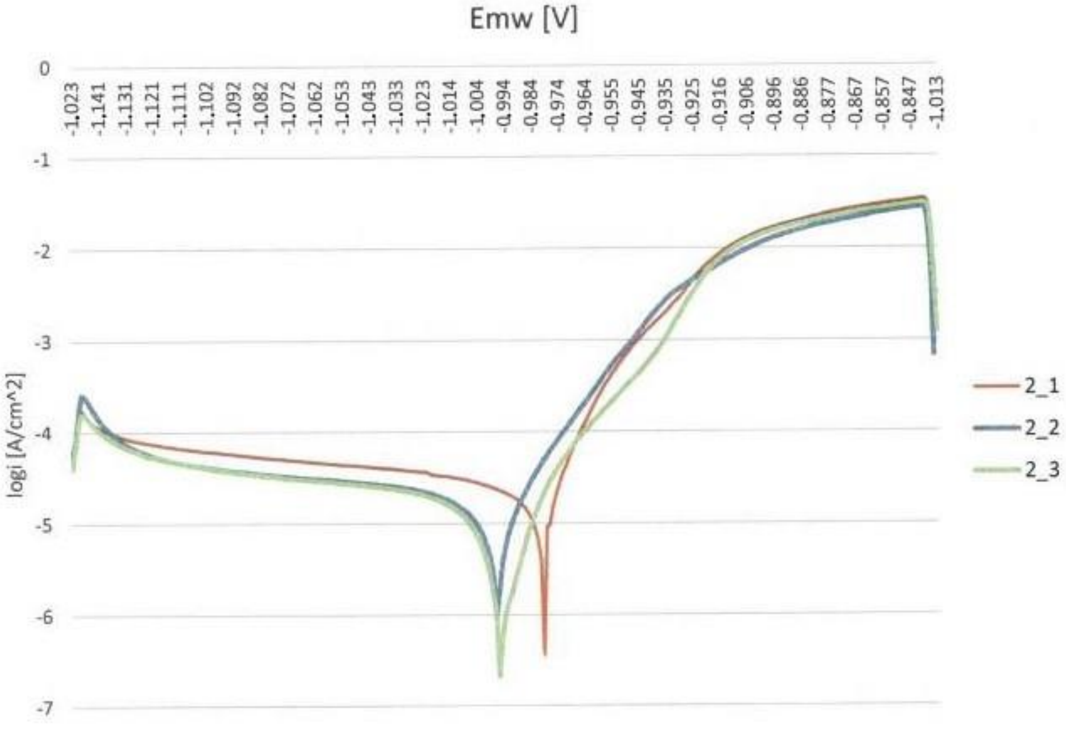

Fig. 10. Summary of the results of the potentiodynamic study of joint 2: 2_1 the first measurement, 2_2 the second measurement, 2_3 the third measurement

Based on the results of the polarization resistance tests, it can be concluded that the joint welded with the linear energy of 0.3 kJ/mm shows a much higher corrosion resistance than those obtained as a result of increasing the linear welding energy to 0.45 kJ/mm. Based on the metallographic analysis and literature data, it can be concluded that the reason for this is the difference in the structure of the welded joint. Joint 1 is characterized by a ferritic-pearlitic structure, the two-phase nature of which works unfavorably for the corrosion resistance in specific conditions. Cementite Fe_3C in relation to ferrite is a cathodic phase, as a result of which the preferential dissolution of ferrite is observed [16-18]. The authors of work [19] showed, that on the surface of cementite, an amorphous and tight layer of corrosion products is formed at room temperature, which is an effective barrier for chloride ions. Increasing the ferrite content, identified in joint 2, results in a decrease in the polarization resistance value, which results in a decrease in corrosion resistance.

The corrosion resistance test was also carried out in a salt spray chamber in accordance with the PN-EN ISO 9227 standard. The samples were placed in a salt chamber for 96 hours, where they were exposed to a 5% of the fog of a salt water solution of sodium chloride at a temperature of 35°C, Fig. 11. Corrosion changes of the tested samples were assessed gravimetrically on the basis of their mass loss and mass loss relative to the surface, table 5. The weight loss of the samples subjected to the corrosion resistance test in the salt spray chamber was small and amounted to a maximum of 2.44 g/m^2 after 96 hours. In accordance with the PN EN 9227 standard, for galvanized samples, the loss values below 50 ± 25 g/m^2 after 48h are correct.

Fig. 11. View of the samples during the salt spray test after 96h

Table 5. Test results

Weld design.	Changing the weight of the sample Δg [g]	Weight Loss Vc [g/m^2day]	Linear corrosion rate Vp [mm/ year]	Corrosion resistance classification
Joint 1	0.1559	2.44	0.1146	Designation IV, °k 6
Joint 2	0.1130	2.04	0.0930	Designation III, °k 5

As a result of the corrosion resistance tests it was found that joint 2 (higher linear energy) had better corrosion resistance. The parent material is classified to the group of resistant materials, material designation III, corrosion resistance grade 5. The zinc coating with a lower corrosion potential than the base material, which was a protector, was more evenly applied to the base material in the tested sample and was an effective barrier against chloride ions. The damage of this coating does not cause environmental attack on the substrate material, a favorable situation of large anodic coating (zinc) and small cathode (substrate) arises.

In order to determine the type and nature of corrosion damage, surface morphology tests of the samples after corrosion tests were carried out using a ZEISS SteREO Discovery V12 stereoscopic microscope. The methodology used allows for a proper assessment of the durability of the applied anti-corrosion protection. The first corrosion damage was observed in the tested samples after 48 hours of exposure to 5% NaCl. After 96 hours, the samples were cleaned and photographs with using a stereoscopic microscope. In joint 1, there was probably a localized attack of the corrosive environment, which resulted in local defects in the material – pinholes. The damage caused by pitting corrosion is observed in the base material and in the weld, Fig 12, in which a significant defect was found.

Based on the observations, it was found that general corrosion was observed in joint 2 and is the result of the action of corrosion microcells occurring on the entire surface of the sample, Fig. 13. In addition, an attack on the weld can be seen, but it did not cause its loss.

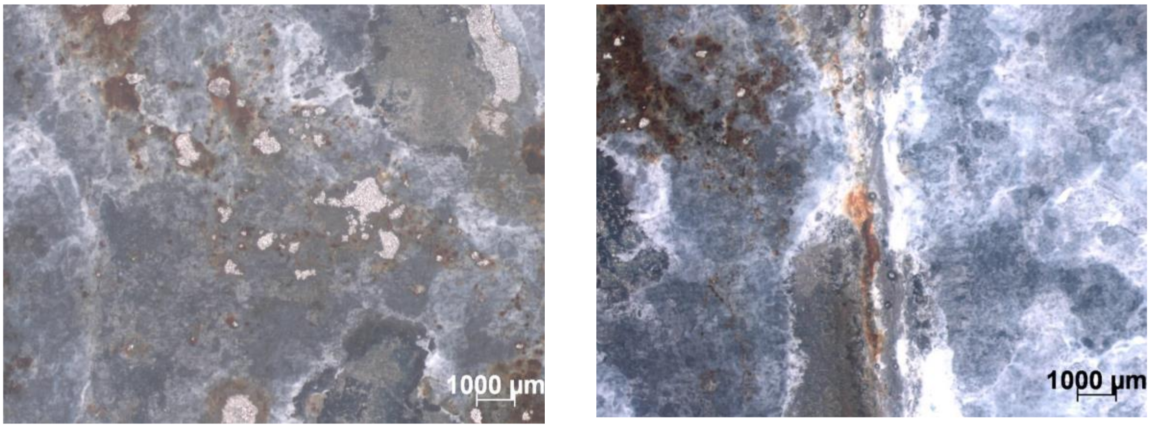

Base material The weld and HAZ

Fig. 12. View of joint 1 after 96 hours of exposure in a salt spray chamber

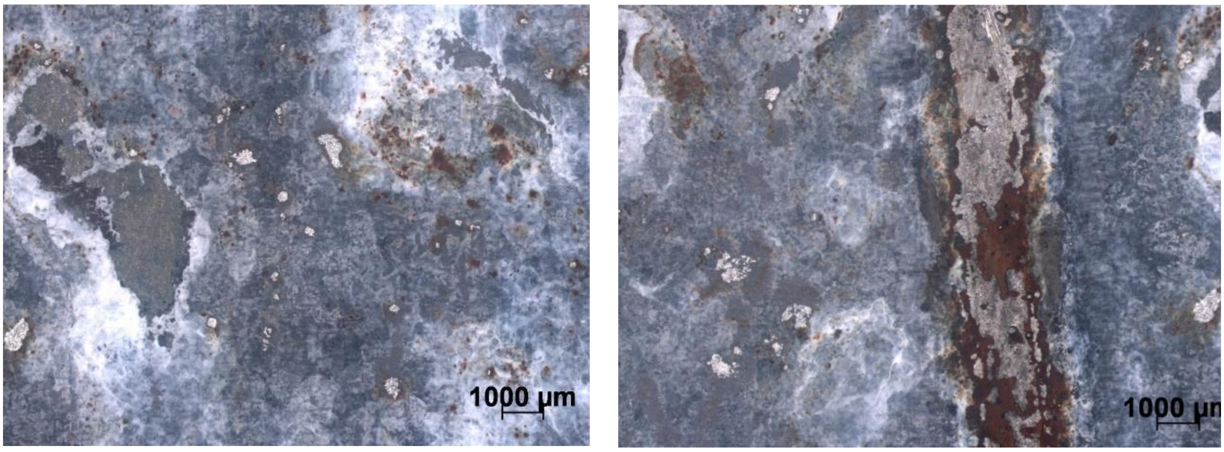

Base material The weld and HAZ

Fig. 13. View of joint 2 after 96 hours of exposure in a salt spray chamber

4. CONCLUSIONS

The tests of laser beam welded joints of galvanized sheets made of DC04 low-carbon steel, 1.0 mm thick, have shown that it is possible to make joints according to ISO 15614-11. Both made joints, regardless of the applied linear welding energy, are characterized by high strength and plastic properties. The analysis of macrostructures of the samples made it possible to determine the influence of the welding parameters on the geometric dimensions of the welds.

It can be noticed that with the increase of the welding linear energy from 0.30 to 0.45 kJ/mm, the weld and the heat affected zone of the welded joints are enlarged. Microscopic examinations showed a fine-grained structure of the parent material and grain growth within the HAZ. The results of microscopic examinations confirmed the hardness measurements. The highest hardness value was obtained in the weld of joint 1 made with lower linear energy (0.3 kJ/mm).

With the increase of the welding linear energy, the value of the maximum hardness in the weld decreases to about 150 $HV_{0.2}$. In the area of HAZ, the obtained hardnesses are in the range of 125 to 145 $HV_{0.2}$ and decrease with the increase of welding linear energy, which is related to the grain size. In the static tensile test, the breakage occurred in the parent material, regardless of the value of the welding linear energy, which confirms the high strength properties of the joints. The tensile strength was in the range of 298 - 301 MPa. In the bending test, regardless of the value of the linear welding energy, a bending angle of 180° was achieved, without cracks. Relative elongation values ranged from 38% to 42%, which confirms high plastic properties. Electrochemical tests showed different corrosion resistance to the environment of chloride ions. On the basis of the obtained corrosion parameters: polarization resistance and corrosion potential, it was shown that welded joint 1 is characterized by better corrosion resistance than joint 2. This is a consequence of the metallographic structure which plays a significant role in the mechanisms and rate of corrosion. Joints with different grain size and different distribution of individual phases were tested. It was found that the fine-grained material of the joint 1, with regular distribution of ferrite and pearlite, is more corrosion resistant than the coarse-grained material with a structure dominated by ferrite, which has a higher electrochemical potential than the cementite in pearlitic grains. The experiment carried out in the salt spray chamber is a control test, often used to determine the quality of a technological process, for example for elements covered with anti-corrosion layers, or to verify the parameters of welded joints. Tests carried out in neutral salt spray show that joint 1, made at a higher welding speed, has worse corrosion resistance than the second joint. The reason for this may be the unevenness of the applied zinc coating or its degradation during welding.

REFERENCES

1. Pawar, N., (2019). *Automotive Advanced High Strength Steel (AHSS)*, Market Professional Survey Report 2019; Analytical Research Cognizance (ARCX001), GrandResearchStore: New York, USA, 101.
2. *DOCOL the Automotive Steel. In The Most Sustainable Solution: Setting the New Standard for the Automotive Industry* (2019) SSAB: Sweden.
3. Ma, J., et al., (2013). *Two-pass laser welding of galvanized high-strength dual-phase steel for a zero-gap lap joint configuration*, Journal of Materials Processing Technology, 213, 495– 507.
4. Reisgen, U., et al., (2010). *Shielding gas influences on laser weldability of tailored blanks of advanced automotive steels*, Applied Surface Science, 257, 1401–1406.
5. Mei, L., et al., (2009). *Research on laser welding of high-strength galvanized automobile steel sheets*, Optics and Lasers in Engineering, 47, 1117–1124.
6. Węgrzyn, T., at al. (2010). *Oxide inclusions in steel welds of car body*, Materials Science Forum, 6, 585-591.
7. Chen, Z., et al., (2014). *A study of fiber laser welding of galvanized steel using a suction method*, Journal of Materials Processing Technology, 214, 1456–1465.
8. Żuk, M., Górka, J., Czupryński, A., Adamiak, M., (2016). *Properties and structure of the weld joints of quench and tempered 4330V steel*, Metalurgija, 55, 613-616.
9. Lifang, M., et al., (2012). *Comparative study on CO_2 laser overlap welding and resistance spot welding for galvanized steel*, Materials and Design, 40, 433-442.
10. Iqbal, S., et al., (2010). *Dual beam method for laser welding of galvanized steel: Experimentation and prospects*, Optics & Laser Technology, 42, 93–98.
11. Górka J., (2016). *Microstructure and properties of the high-temperature (HAZ) of thermo-mechanically treated S700MC high-yield-strength steel*, Materials and technology, 50, 617–621.
12. Coroado, J., Ganguly, S., Suder, W., Williams, S., Meco, S., Pardal, G., (2021). *Selection of parameters in nanosecond pulsed wave laser micro-welding*, The International Journal of Advanced Manufacturing Technology, 115(9-10), 2929-2944.
13. Dasgupta, A.K., Mazumder, J., (2008). *Laser welding of zinc coated steel: an alternative to resistance spot welding*, Science and Technology of Welding and Joining, 13, 289–293.
14. Górka, J., Stano, S., (2016). *The structure and properties of filler metal-free laser beam welded joints in steel S700MC subjected to TMCP*, Laser Technology 2016: Progress and Applications of Lasers, 183-190.
15. Grajcar, A., Morawiec, M., Różański, M., Stano S., (2017). *Twin-spot laser welding of advanced high-strength multiphase microstructure steel*, Optics and Laser Technology, 52–61.
16. Yumoto, H., Nagamine, Y., Nagahama, J., Shimotomai, M., (2002). *Corrosion and stability of cementite films prepared by electron shower,* Vacuum, 65(3–4), 527-531.
17. Murase, Y., Masuda, H., Katayama, H., (2021). *Corrosion Resistance of Finer/Coarser Pearlitic Structures of Carbon Steel,* Journal of The Electrochemical Society, 168, 1-27.
18. Sánchez, J., Fullea, J., Andrade, C., Gaitero, J., Porro, A., (2008). *AFM study of the early corrosion of a high strength steel in a diluted sodium chloride solution,* Corrosion Science, 50, 1820–1824.
19. Kadowaki, M., et al., (2019). *Anodic polarization characteristics and electrochemical properties of Fe_3C in chloride solutions,* Journal of The Electrochemical Society, 166(12), 345-351.

Received: May 18, 2023/ Accepted: December 15, 2023 / Paper available online: December 20, 2023©
International Journal of Modern Manucaturing Technologies